

Links among extracellular enzymes, lignin degradation and cell growth establish the models to identify marine lignin-utilizing bacteria

Xiaopeng Wang,^{1,2} Lu Lin ^{1*} and Jizhong Zhou³

¹*Institute of Marine Science and Technology, Shandong University, Qingdao, China.*

²*Key Laboratory of Applied Marine Biotechnology, Ministry of Education, Ningbo University, Ningbo, China.*

³*Institute for Environmental Genomics, Department of Microbiology and Plant Biology, and School of Civil Engineering and Environmental Sciences, University of Oklahoma, Norman, OK.*

Summary

A major conundrum in the isolation of prokaryotes from open environments is stochasticity. It is especially difficult to study low abundance groups where very little biological information exists, although single-cell genomics and metagenomics have alleviated some of this bottleneck. Here, we report an approach to capture lignin-utilizing bacteria by linking a physical model to actual organisms. Extracellular enzymes, lignin degradation and cell growth are crucial phenotypes of lignin-utilizing bacteria, but their interrelationships remain poorly understood. In this study, the phenotypes of bacteria isolated from *in situ* lignocellulose enrichment samples in coastal waters were traced and statistically analysed. It suggested cell growth, dye-decolorizing peroxidase (DyP) and reactive oxygen species (ROS) were significantly correlated with lignin degradation, exhibiting a genus-specific property. The established models enabled us to efficiently capture lignin-utilizing bacteria and rapidly evaluate lignin degradation for *Bacillus* and *Vibrio* strains. Through the model, we identified several previously unrecognized marine bacterial lignin degraders. Moreover, it demonstrated that the isolated marine lignin-utilizing bacteria employ a DyP-based system and ROS for lignin depolymerization, providing insights into the mechanism of marine bacterial lignin degradation. Our findings should have

implications beyond the capture of lignin-utilizing bacteria, in the isolation of other microorganisms with as-yet-unknown molecular biomarkers.

Introduction

The isolation and cultivation of novel microorganisms is both laborious and low-throughput. Moreover, the majority of microorganisms remain unculturable (D'Onofrio *et al.*, 2010) and thus, microbial pure culture studies have been neglected in recent years (Cross *et al.*, 2019). With the advance of high-throughput sequencing techniques, single-cell genomes and metagenomes have attracted attention. Culture-independent approaches expand the repertoire of microbial species and alleviate cultivation recalcitrance (Vavourakis *et al.*, 2018; Nayfach *et al.*, 2019). However, it is worth noting that the numerous hypothetical physiological or ecological roles, indicated via such approaches, remain to be validated by physiological and genetic investigation of a pure culture (Lagier *et al.*, 2016). Therefore, the isolation and cultivation of unknown microorganism remains essential in the study of both microbiology and ecology.

One great limitation of cultivation approaches is stochasticity, indicating that the isolation of new microorganisms is driven partly by chance (Cross *et al.*, 2019). As a result, specific groups, especially those with low abundance, cannot be effectively captured from open environments. Taking lignin-utilizing bacteria as an example, a few bacteria from soil and aquatic environments have been isolated and shown to break down lignin as a part of global carbon cycling (Brown and Chang, 2014). In contrast to fungal lignin degradation (Floudas *et al.*, 2012), the study of bacterial lignin degradation, in the form of gene databases, lags far behind (Strachan *et al.*, 2014; de Gonzalo *et al.*, 2016). Consequently, it is hard to identify appropriate molecular biomarkers to screen lignin-utilizing strains via high-throughput omics approaches. On the other hand, traditional selection methods, e.g., cultivation of strains on lignin, cannot be easily monitored in a high-throughput manner by optical density at 600 nm (OD₆₀₀), due to the inherent

Received 23 April, 2020; accepted 18 October, 2020. *For correspondence. E-mail linlu2019@sdu.edu.cn; Tel: 0532 58633267, 0532-58633226; Fax: 0532 58633218.

heterogeneity and recalcitrant chemical structure of lignin (Zhao *et al.*, 2016; Lin *et al.*, 2019). Thus, this strategy is inefficient and laborious. Alternatively, directly linking phenotypes to actual organisms and identifying a physical model may offer clues for the improvement of isolation and cultivation strategies. Bacteria have evolved extracellular oxidative enzymes, such as laccases and heme-containing peroxidases (e.g., DyPs) to initiate lignin decomposition. Laccases are multi-copper oxidases. They employ a cluster of four copper ions and self-generate radicals for phenolic lignin compound oxidations (de Gonzalo *et al.*, 2016; Zhao *et al.*, 2016). On the other hand, peroxidases are also well-known ligninolytic enzymes. Lignin peroxidases (LiPs) and manganese peroxidases (MnPs) activities have been detected in lignin-degrading bacteria, such as *Bacillus* sp. CSA105 (Kharayat and Thakur, 2012), *Enterobacter hormaechei* PY12 (Zhou *et al.*, 2017) and *Comamonas* sp B-9 (Chen *et al.*, 2012), but few of their gene sequences have been reported (de Gonzalo *et al.*, 2016). In addition, DyPs represent a newly discovered family of heme-containing peroxidases and cleave the C_α-C_β linkage of phenolic lignin compounds, requiring hydrogen peroxide (H₂O₂) as an electron acceptor (de Gonzalo *et al.*, 2016; Lin *et al.*, 2019). Moreover, redox systems [e.g., Reactive oxygen species (ROS)] that generate and recycle reactive radicals are commonly required to assist peroxidase-based lignin depolymerization (Bissaro *et al.*, 2018; Becker and Wittmann, 2019). The resulting low-molecular aromatic compounds are subsequently taken up and further catabolized for energy generation to support cell growth (Salvachua *et al.*, 2015; Lin *et al.*, 2019). Therefore, the phenotypes of extracellular enzymes, lignin degradation and cell growth are thought to be closely related in lignin-utilizing bacteria. Numerous studies have suggested that this close relationship could be utilized to isolate lignin-degrading bacteria (Bandounas *et al.*, 2011; Wang *et al.*, 2016; Yang *et al.*, 2017; Velayutham *et al.*, 2018); however, few have attempted to untangle the links among these phenotypes. The complex relationship of these factors undoubtedly represents a major hurdle in the isolation, cultivation and investigation of lignin-utilizing bacteria. Exploration of the links among these three phenotypes to establish physical models should be a rational strategy to effectively capture and culture lignin-utilizing bacteria from the open environment.

In this study, *in situ* straw lignocellulose enrichments were performed in coastal waters of the East China Sea to enhance the abundance of lignin-utilizing bacteria in the local microbial community. Forty-nine bacterial strains from 200 isolates were collected to trace their phenotypes under different culture media. Discriminant function analysis and linear regression analysis were carried out to reveal the relationship of extracellular enzymes, cell

growth and lignin degradation. These findings established models to simply and efficiently distinguish lignin-utilizing strains and to evaluate the lignin degradation capabilities of *Bacillus* and *Vibrio* strains. Moreover, in contrast to other extracellular enzymes, DyP-type peroxidases, together with reactive ROS, are primarily responsible for soluble and insoluble lignin degradation, suggesting novel clues to investigate the mechanisms of marine bacterial lignin degradation.

Results

The diversity of bacterial isolates with lignin-degrading abilities from in situ lignocellulose enrichment samples in coastal waters of the East China Sea

A total of 200 isolates were picked from *in situ* lignocellulose enrichment samples in coastal waters of the East China Sea (Fig. S1). These isolates were cultured in 2216E liquid medium to monitor their cell growth (as measured by OD600) and investigate four types of extracellular ligninolytic enzymes, DyP, MnP, LiP and laccase at early-, mid-, and late-log phases. 2, 6-Dimethylphenol (2, 6-DMP) was utilized as the catalytic substrate to measure laccase activity, while 2, 6-DMP and H₂O₂ were employed to detect DyP activity. 2, 6-DMP and MnSO₄ with H₂O₂ were utilized to investigate MnP activity, while veratryl alcohol (VA) with H₂O₂ was employed to measure LiP activity. Furthermore, the 16S rRNA genes from 200 isolates were amplified by PCR and sequenced. Isolates with identical 16S rRNA sequence and similar growth and extracellular ligninolytic enzyme activities curves were identified as belonging to the same group (Figs. S2 and S3). As a result, all isolates were classified into 49 groups, each represented by a single strain, which belonged to 28 species from 15 genera (Fig. 1 and Table S1). Of these, strains from the *Bacillus* and *Vibrio* genera, which are widely distributed in offshore marine environments (Shobharani *et al.*, 2015; Baker-Austin *et al.*, 2018), were the major members, accounting for 22% and 16% of the 49 representative strains respectively (Fig. 1).

Of the 49 representative strains, 37 showed positive growth in soluble lignin mineral medium, indicating that they could utilize soluble lignin as the sole carbon source and represented lignin-utilizing strains (Fig. 1 and Table S2). A subset of 29 strains further exhibited positive growth in insoluble lignin mineral medium, suggesting they are able to utilize different types of lignin (Fig. 1 and Table S3). Among the 12 strains that could not grow in soluble lignin mineral medium, six strains were identified to be capable of soluble lignin degradation when they were cultured in mineral medium supplemented with glucose and soluble lignin as co-substrates (Fig. 1 and Table S4). They were, hence, designated as lignin-degrading strains.

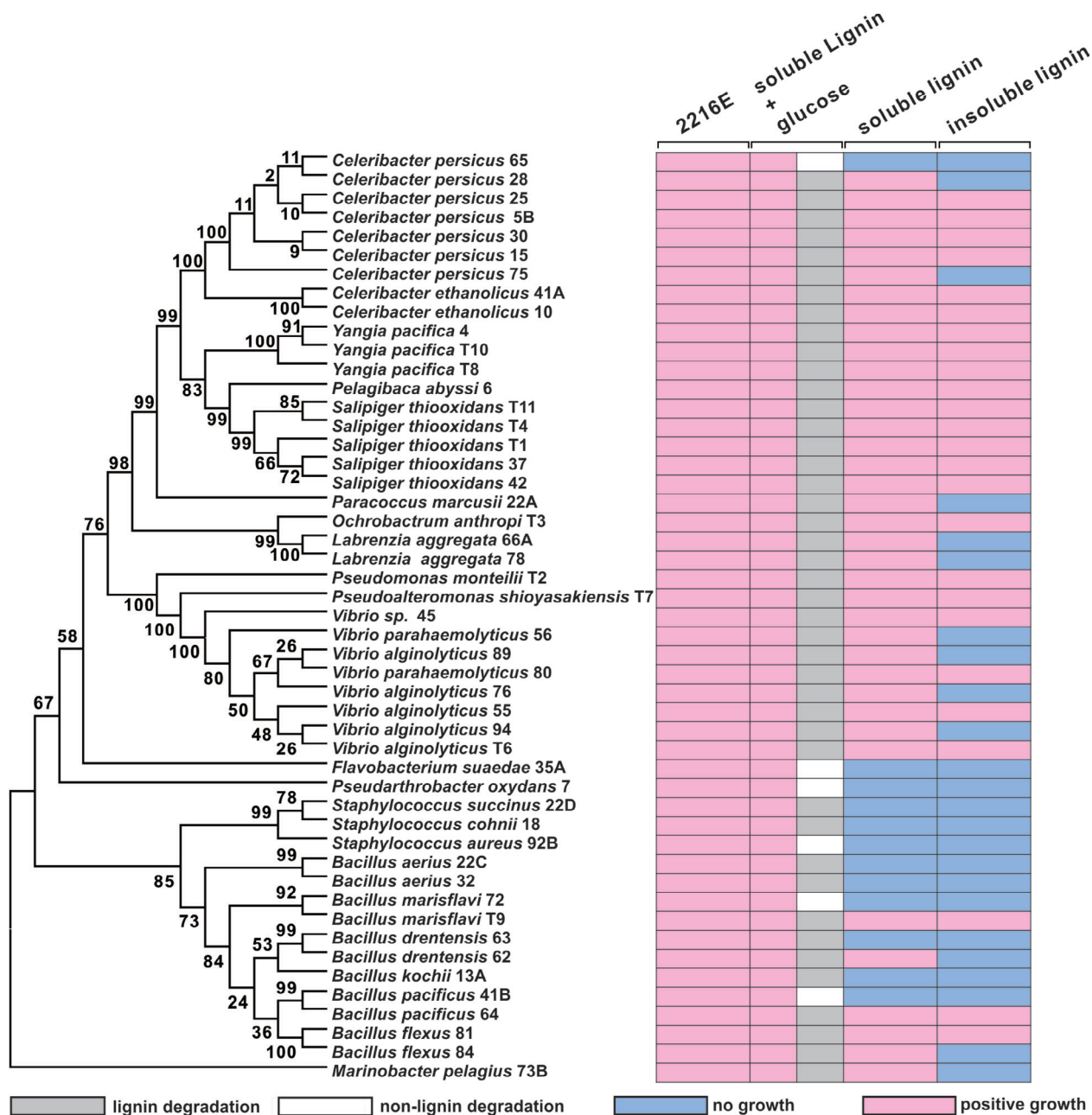


Fig. 1. Phylogenetic tree and carbon utilization patterns of the isolated strains. All strains were cultured in 2216E medium, soluble lignin mineral medium with glucose, soluble lignin mineral medium and insoluble lignin mineral medium respectively. Phylogenetic trees were constructed by the Neighbour-Joining method using full length sequences of the 16S rRNA gene. The percentage of replicate trees is indicated at the branch nodes. [Color figure can be viewed at wileyonlinelibrary.com]

Bacterial extracellular enzyme activities and cell growth in 2216E medium can be employed to distinguish whether strains can utilize lignin as a sole carbon substrate

Out of the 49 strains, 37 showed positive growth on lignin and 12 exhibited no growth. Descriptive statistics of these 49 strains were analysed for the four types of extracellular enzyme activity and OD600 values during late-log phase in 2216E medium. The results suggested that

positive growth strains have higher mean values than no growth strains for all extracellular enzyme activities; however, OD600 showed the opposite (Fig. 2A). Moreover, significant differences in DyP ($p = 0.03$), MnP ($p < 0.005$) and OD600 ($p = 0.02$) parameters between the two strain types were observed (Fig. 2A and Table S5). Subsequently, multivariate discriminant function analysis of these five variables was performed to efficiently identify lignin-utilizing strains. As a result, a significant statistical

model ($p < 0.005$) was consequently proposed: Y1 (lignin utilization strains) = $0.659 \times \text{DyP} + 7.658 \times \text{MnP} + 4.888 \times \text{LiP} + 0.843 \times \text{OD600} + 6.623 \times \text{Laccase} - 2.754$ and Y2 (non-lignin utilization strains) = $-0.041 \times \text{DyP} + 2.055 \times \text{MnP} + 0.400 \times \text{LiP} + 1.924 \times \text{OD600} - 1.309 \times \text{Laccase} - 4.887$, where, DyP, MnP, LiP, Laccase activities (U/ml of cell culture) and OD600 value were measured during the late-log phase when a bacterial strain was cultured in 2216E medium at 30°C (Table S1). Thus, for an unknown marine bacterium, Y1 and Y2 values are subsequently calculated respectively. If Y1 is greater than Y2, the strain is predicted to be a lignin-utilizing strain. Otherwise, it is believed the strain is incapable of growth on lignin.

Moreover, the multivariate discriminant function analysis suggested that OD600 was the most important variable, followed by DyP-type peroxidase activity (Fig. 2B). To further validate the impact of each variable on the accuracy of this discriminant model, stepwise discriminant function analysis was performed. The results suggested that when just two variables, DyP-type peroxidase and cell growth, were considered, the model was still significant ($p < 0.005$). Hence, employing the two variables, the statistical model was simplified and shown below: Y1 (lignin-utilizing strains) = $0.592 \times \text{DyP} + 0.874 \times \text{OD600} - 1.890$, Y2 (non-lignin-utilizing strains) = $-0.051 \times \text{DyP} + 1.920 \times \text{OD600} - 4.844$.

Next, to examine the accuracy of these proposed models, cross-validated classification analysis was firstly performed, where each sample from these 49 strains was treated as a validation set, and classified by discriminant functions created by the training set of all individuals except itself. The accuracies of cross-validation were 85.7% for the multivariate discriminant function analysis

and 89.8% for the stepwise discriminant function analysis respectively (Table 1). Moreover, as an additional test, 27 bacterial strains, which were isolated from different marine environments (e.g., cold springs, coastal areas, and marine sediments) in our lab, were randomly selected to test the models. They were cultured in 2216E medium at 30°C to investigate the four types of extracellular enzyme activities and OD600 values during late-log phase (Fig. S4 and Table S6). Y1 and Y2 values were subsequently calculated based on the models respectively. The results suggested that the accuracy of multivariate discriminant function analysis was 81.5%, while the accuracy of stepwise analysis was 88.9%, similar to that of the cross-validated classification analysis (Table 1). These results validated the viability of the discriminant models.

Taken together, the four types of extracellular enzyme and OD600 value in 2216E medium are all significantly associated with bacterial lignin utilization. Of them, DyP-type peroxidase and OD600 value are the most importance variables. The model, via the two variables, was proposed to effectively distinguish between the lignin utilization strains and strains incapable of lignin utilization, for its simplicity and slightly higher accuracy.

Cell growth in lignin mineral medium significantly correlates with lignin utilization

Through the discriminant model, we can easily and effectively identify lignin utilization strains. To further reveal the quantitative relationships of extracellular enzymes activities, cell growth and lignin degradation, linear regression analysis was carried out on strains cultured in soluble lignin mineral medium. Moderate association

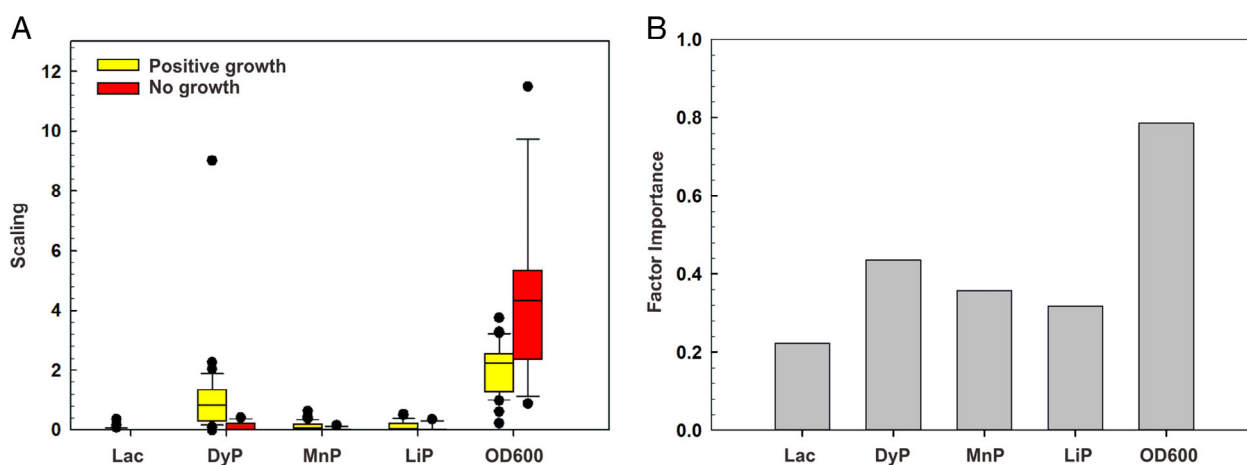


Fig. 2. Discriminant function analysis for those lignin-utilizing strains and non-lignin-utilizing strains. A. Multivariate discriminant function analysis revealed different patterns for the four types of extracellular enzyme activities and cell growth in 2216E medium between lignin-utilizing strains and non-lignin-utilizing strains. B. Bar graph showing the importance of each variable in associations with lignin utilization. [Color figure can be viewed at wileyonlinelibrary.com]

Table 1. Classification accuracy of OD600 and enzyme activity parameters in bacterial lignin degradation by discriminant function analysis.

Functions		Positive growth ^a	Non-growth ^a	Accuracy (%)
Established model (49 strains)	Function 1: Multivariate analysis			
	Original	35/37 (94.6%)	9/12 (75%)	85.7
	Cross-validated	33/37 (89.2%)	9/12 (75%)	
	Function 2: Stepwise analysis			89.8
Original	36/37 (97.3%)	8/12 (66.7%)		
Model application (27 strains)	Function 1: Multivariate analysis			
	Original	19/20 (95.0%)	3/7 (42.9%)	81.5
	Function 2: Stepwise analysis			88.9
	Original	20/20 (100.0%)	4/7 (57.1%)	

^aPredicted group membership/actual group membership.

between cell growth [as measured by colony forming units/mL (CFUs/ml)] and lignin degradation was found (correlation coefficient $R = 0.39$, $p = 0.02$, Fig. S5). When DyP-type peroxidase was introduced as another independent variable, such moderate association with lignin utilization was improved (correlation coefficient $R = 0.47$, $p = 0.003$, Fig. 3A). Between these two variables, cell growth was the most important factor, followed by DyP (Fig. 3A).

Considering that bacteria in different genera potentially have divergent lignin degradation properties, two dominant genera among the isolated strains, *Bacillus* and *Vibrio*, were chosen for linear regression analysis. As expected, higher correlation with lignin degradation was observed (correlation coefficient $R = 0.79$, $p < 0.005$, Fig. 3B). Under this condition, the plot equation was defined as: lignin degradation (%) = $(2.675E-12 \times CFU_{max} - 0.113 \times DyP + 0.210) \times 100$, where, DyP was measured at the stationary phase when either a *Bacillus* or *Vibrio* strain was cultured in soluble lignin mineral medium at 30°C, and CFU_{max} was the maximum CFU value during the cultivation. To validate this linear regression model, the lignin consumptions of five *Bacillus* or *Vibrio* strains, from the 27 tested marine bacteria, were calculated via the equation. Meanwhile, their actual lignin consumptions were experimentally measured (Table S7). As expected, similar correlation ($R = 0.74$) with lignin degradation was observed (Fig. 3C).

Together, our results demonstrated two aspects. First, lignin degradation is moderately associated with cell growth and DyP-type peroxidase in soluble lignin mineral medium. Moreover, cell growth is not the only variable that reveals links with lignin degradation, although it is the most important factor. Second, when only members of the genera *Bacillus* and *Vibrio* are considered, such association can be enhanced, suggesting that the three physiological phenotypes could have genus-specific properties.

Compared to three other types of extracellular ligninolytic enzymes, DyP-type peroxidase is significantly associated with lignin degradation

As mentioned previously, DyP-type peroxidase activity has significant correlation with lignin degradation (Fig. 3A–B). Because enzyme activity is ambivalent under different conditions (e.g., enzyme production conditions and enzyme activity assay conditions) (Agrawal and Verma, 2019), it may hamper uncovering the links among the three physiological phenotypes. Thus, extracellular ligninolytic enzymes activities under different conditions (media and enzyme catalytic substrates) were investigated to minimize the ambivalence. For this purpose, enzymes were monitored in three different growth media, 2216E and soluble/insoluble lignin mineral media. Furthermore, another commonly reported catalytic substrate, 2, 2'-azino-bis (3-ethylthiazoline-6-sulfonate) (ABTS) (Brown *et al.*, 2012), was employed to measure DyP-type peroxidase and laccase activity, respectively, in addition to the previously utilized 2, 6-DMP.

To begin, DyP-type peroxidases exhibit less specificity to catalytic substrates, whereas laccases show specificity to ABTS. When the 49 strains were cultured in 2216E medium, 39 strains showed DyP-type peroxidase activity via 2, 6-DMP substrate with H_2O_2 , whereas 38 strains exhibited activity by ABTS substrate with H_2O_2 (Table 2 and Table S1). Highly significant correlation of DyP-type peroxidase activity between the two catalytic substrates was observed (correlation coefficient $R = 0.90$, $p < 0.005$, Fig. 3D). Similarly, moderate correlation of DyP-type peroxidase activity between the two catalytic substrates was found when strains were grown in either soluble lignin mineral medium or insoluble lignin mineral medium (correlation coefficient $R = 0.50$ – 0.52 , $p < 0.05$, Fig. S6A and B and Table 2). This suggested that DyP-type peroxidase activities were relatively stable under the two different catalytic substrates, although DyP-type peroxidase activities detected by ABTS were higher than those by

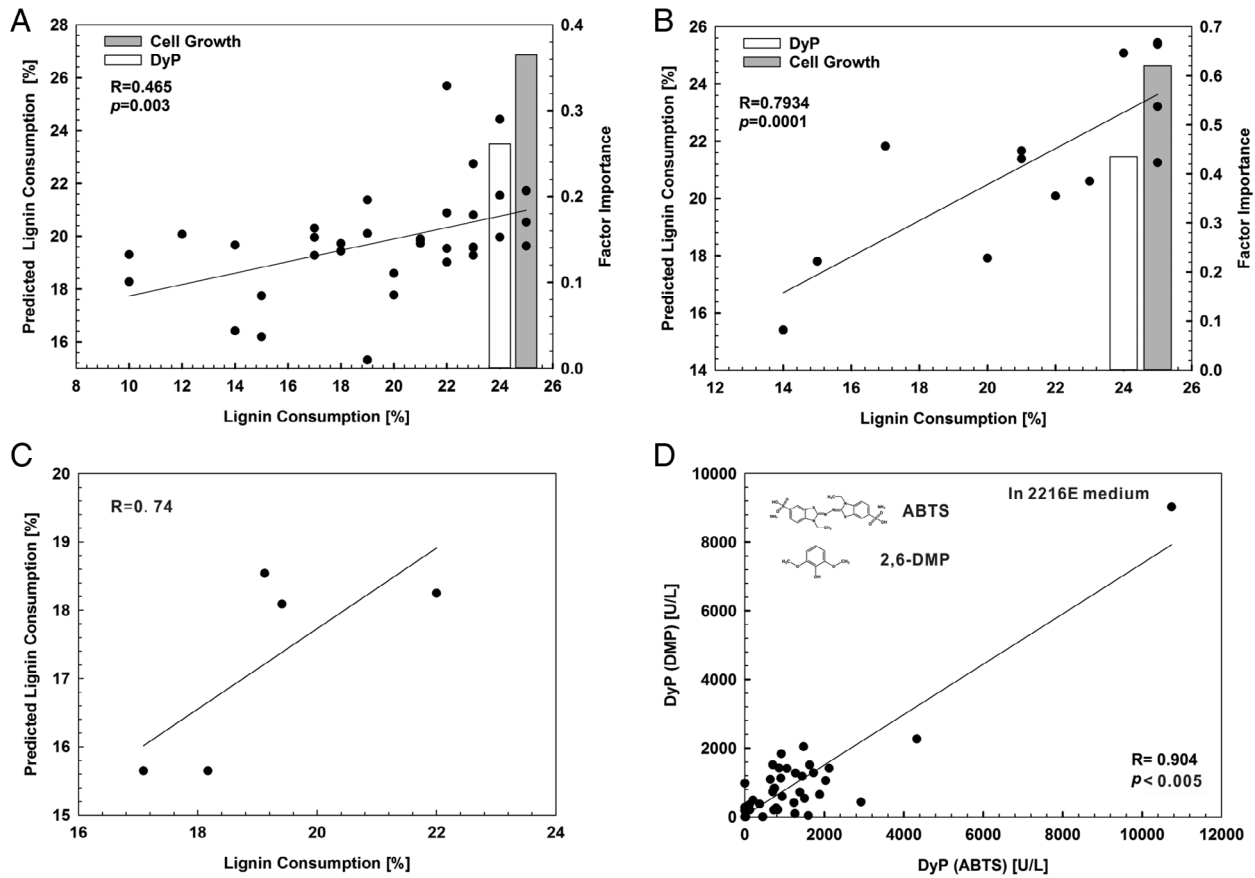


Fig. 3. Linear regression analysis for the correlation among lignin degradation, DyP-type peroxidase activity and cell growth. A. DyP-type peroxidase activity and cell growth of the 37 strains capable of growth on soluble lignin, as two independent variables, are significantly associated with lignin utilization. B. Correlation between lignin utilization and DyP-type peroxidase activity plus cell growth for strains belonging to the genera *Bacillus* and *Vibrio*. C. Correlation between lignin utilization and DyP-type peroxidase activity plus cell growth for the *Bacillus* and *Vibrio* strains from the 27 tested strains. D. Correlation between DyP-type peroxidase activities in 2216E medium as measured by ABTS and 2, 6-DMP assays.

Table 2. Comparison of enzyme profile under different culture conditions.

Medium	Total strains	Lac (ABTS) ^a		DyP (ABTS) ^a		Lac (DMP) ^a		DyP (DMP) ^a		MnP		LiP	
		Strains	Ratio (%)	Strains	Ratio (%)	Strains	Ratio (%)	Strains	Ratio (%)	Strains	Ratio (%)	Strains	Ratio (%)
2216E soluble lignin	49	18.0	36.7	38.0	77.6	10.0	20.4	39.0	79.6	33.0	67.3	28.0	57.1
mineral medium	37	25.0	67.6	37.0	100.0	7.0	18.9	31.0	83.8	0.0	0.0	0.0	0.0
insoluble lignin	25	1.0	4.0	25.0	100.0	1.0	4.0	24.0	96.0	0.0	0.0	0.0	0.0
mineral medium													

^aThe catalytic substrate was utilized to measure enzyme activity.

2, 6-DMP (Fig. 3D and Table S1–S3). In contrast, laccases presented the opposite results. In 2261E medium, of the 49 strains, only 10 strains showed laccase activity via 2, 6-DMP substrate, whereas

18 strains exhibited laccase activity with ABTS as the substrate. Similar results were observed in soluble lignin medium (Table 2). This demonstrated that laccase activity was more sensitive to ABTS, compared to that of

2, 6-DMP (Table 2). Moreover, non-significant correlation of laccase activity between the two catalytic substrates was observed, when strains were grown in either 2216E medium or soluble lignin mineral medium. Thus, laccase activity showed ambivalence under the two substrates.

Second, DyP-type peroxidases play a key role in degrading two types of lignin. As previously stated, Laccase, DyP, LiP and MnP activities were monitored when strains were cultured in the three different media respectively (Table 2 and Table S1–S3). Unexpectedly, MnP and LiP activities were only observed in 2216E medium. When strains were grown in (soluble and insoluble) lignin mineral media, none showed MnP and LiP activities, indicating that unlike fungi (Bugg *et al.*, 2011), these bacteria possibly do not employ MnP and LiP to depolymerize lignin. In contrast, 83.8–100% of strains had DyP-type peroxidase activity in (soluble and insoluble) lignin mineral media via ABTS or 2, 6-DMP substrate, respectively, revealing that DyP-type peroxidases appear to be the major ligninolytic enzymes for the lignin depolymerization (Table 2). Furthermore, DyP-type peroxidase activities in soluble lignin mineral medium showed significant association with the same activities in insoluble lignin medium ($R = 0.43$, $p = 0.037$, Fig. S6C). Therefore, even though different types of lignin were utilized, the expression pattern was relatively consistent, further validating its key role in lignin degradation.

Third, laccases possibly assist lignin degradation. Of the 37 strains that were able to grow in soluble lignin mineral medium, seven and 27 strains, with DMP and ABTS, respectively, showed laccase activity (Table 2). Furthermore, when strains were cultured in insoluble lignin mineral medium, only one strain, *Ochrobactrum anthropi* T3, showed laccase activity (Table 2 and Table S3). Hence, laccase is unlikely to be essential in marine bacterial lignin degradation, especially for insoluble lignin.

ROS is an essential factor in lignin degradation, when bacteria employ a DyP-based enzymatic system

As stated earlier, DyP-type peroxidases were significantly associated with lignin degradation. It is worth noting that ROS is required for effective peroxidase-based lignin degradation (de Gonzalo *et al.*, 2016). This involves the redox cycling process, where hydroxyl radicals are generated from H_2O_2 after a single-electron reduction [e.g., by Fe(II) in fenton reaction] to attack C-C linkages in lignin (Fig. 4A) (Lin *et al.*, 2016; Bissaro *et al.*, 2018). The ROS, therefore, might be another parameter that should be considered to further reveal links among the three physiological phenotypes.

For this purpose, two typical groups of strains were tentatively selected to investigate the extracellular ROS concentration. The two strains within each group showed

similar increased folds of CFUs and DyP-type peroxidase activity ($p > 0.05$), but significantly different lignin degradation when cultured in soluble lignin medium ($p < 0.05$). Group I contained *Bacillus flexus* 81 and *Pseudoalteromonas shioyasakiensis* T7. When they were compared, they showed similar cell growth ($p = 0.14$) and peroxidase activity ($p = 0.75$, Fig. 4B). However, *B. flexus* 81 degraded 14.52% lignin, while *P. shioyasakiensis* T7 utilized 9.88% lignin ($p < 0.005$, Fig. 4B). ROS assay suggested that *B. flexus* 81 had a higher (4.25-fold) extracellular ROS concentration than that of *P. shioyasakiensis* T7, consistent with the observed lignin degradation ($p = 0.03$, Fig. 4B). In group II, *B. flexus* 84 and *Salipiger thiooxidans* 37, also showed similar result. *B. flexus* 84 produced 9.92-fold higher ROS and degraded 1.63-fold more lignin, compared to *S. thiooxidans* 37 ($p < 0.005$), even though they had similar DyP-type peroxidase activity and cell growth ($p > 0.05$, Fig. 4B). These results indicated ROS contributed to lignin degradation. To further validate this hypothesis, the extracellular ROS concentrations of *Bacillus* and *Vibrio* strains were measured and introduced into the linear regression analysis as the third independent variable. As expected, the associated correlation with lignin degradation was improved ($R = 0.85$, $p < 0.005$), compared to when only two variables were considered (Fig. 4C and Fig. 3B). Moreover, ROS is the second most important variable, followed by cell growth, to predict lignin degradation (Fig. 4C). Hence, the final lignin degradation plot equation for *Bacillus* and *Vibrio* strains was defined as: lignin degradation (%) = $2.092E-12 \times CFU_{max} + 3.146E-05 \times ROS - 0.007 \times DyP + 0.180$. As a result, five *Bacillus* or *Vibrio* strains from the 27 tested marine bacteria were cultured in soluble lignin mineral medium at 30°C. The DyP activity and ROS during the stationary phase, as well as the maximum CFU value (CFU_{max}) of each strain, was measured (Table S7). The correlation between calculated lignin consumption and actual values was 0.86, which is comparable with the linear regression model (Fig. 4D).

Discussion

Targeted isolation of lignin-degrading bacteria is the key first step to study their role in global carbon source and biomass utilization. However, limited molecular biological information and laborious cultivation work restrict study to a narrow range of lignin-degrading bacteria strains with well-established biological backgrounds (Becker and Wittmann, 2019; Lin *et al.*, 2019). Extracellular ligninolytic enzymes activity, cell growth and lignin degradation are crucial traits during bacterial lignin degradation. Testing the links among these three phenotypes serves as an essential foundation in isolating

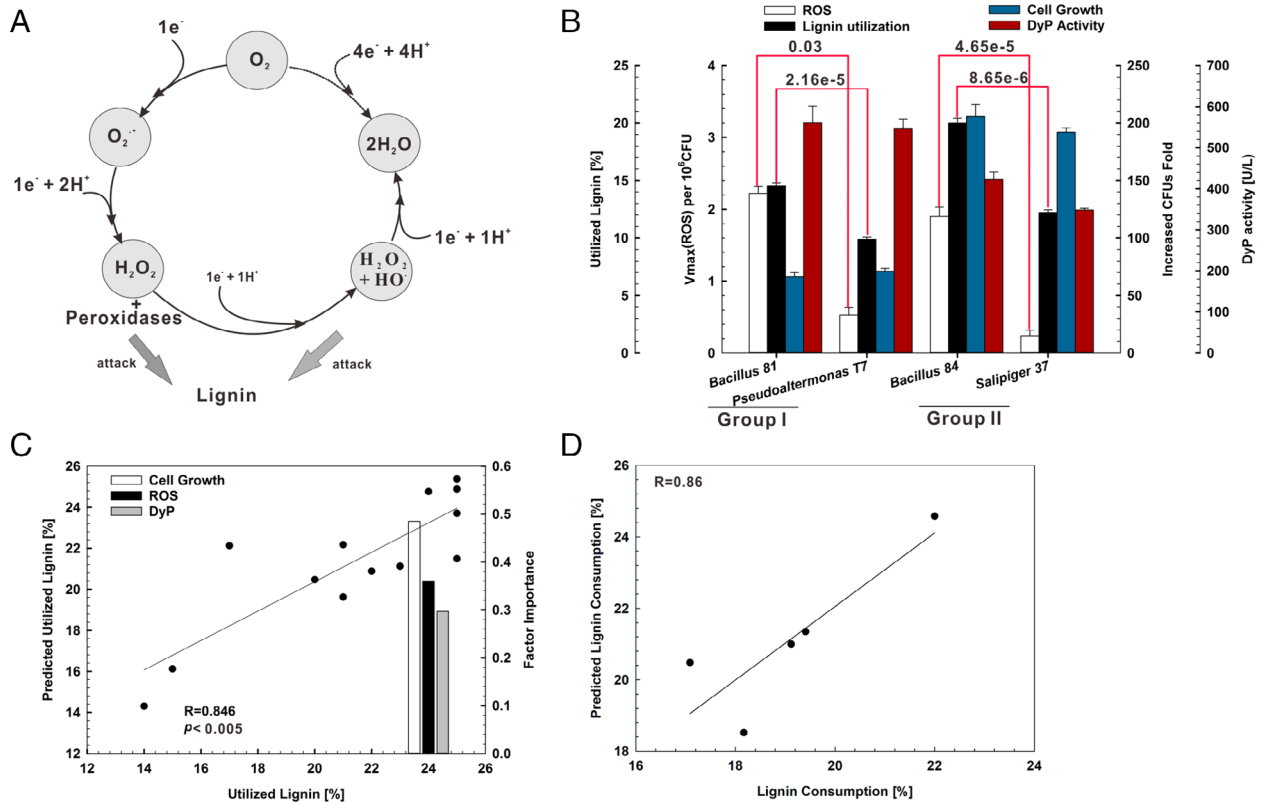


Fig. 4. ROS is the key factor to evaluate the lignin degradation. A. The redox cycling process of ROS from molecular oxygen (O_2) to water (Bissaro *et al.*, 2018). B. Strains with similar cell growth and DyP-type peroxidase activity showed significantly different ROS formation rate and lignin degradation. Maximum rate of ROS formation in culture supernatant for 90 min was evaluated by CM-H2DCFDA fluorescence assay. Differences between groups were evaluated using two tailed unpaired *t*-tests. For selected pairs that exhibited significant differences, *p*-values are shown (those with < 0.05 are considered significant). C. Correlation among lignin degradation, DyP-type peroxidase activity, ROS and cell growth for those *Bacillus* and *Vibrio* strains. D. Application of lignin degradation model in the *Bacillus* and *Vibrio* strains from the 27 tested strains. [Color figure can be viewed at wileyonlinelibrary.com]

lignin utilizing bacteria as well as understanding the mechanism of lignin biodegradation.

Features of discriminant model to discriminate lignin-utilizing bacteria

Our study constructed a simple and productive discriminant model to clarify the complex relationship among phenotypes (Fig. 5A and B). This model enabled us to rapidly and efficiently identify lignin-utilizing strains. We initially screened lignin-degrading strains by ligninolytic indicators (e.g., thiazine dye methylene blue, the anthraquinone dye remazol brilliant blue R and guaiacol), according to previously reported strategies (Bandounas *et al.*, 2011; Wang *et al.*, 2016). However, some strains with positive colour reaction effects either did not degrade lignin or exhibited negative extracellular enzyme activity. In contrast, some with negative colour reaction were found to be capable of growth on lignin (data not shown). These types of results greatly interfere with our ability to

screen lignin-degrading strains. Reliable results can be obtained by cultivation of strains on lignin. However, the cell growth cannot be easily monitored in a high-throughput manner by optical density at 600 nm (OD600) (Zhao *et al.*, 2016; Lin *et al.*, 2019). Furthermore, longer growth periods under lignin substrate and cumbersome procedures to detect lignin degradation largely limited this strategy in a low-throughput and laborious manner. Here, we captured that extracellular enzyme activities and OD600 values in 2216E medium exhibited the distinct patterns between strains able to utilize lignin and those that cannot, demonstrating that these two types of strains have different physiological features, even when lignin is absent (Fig. 2A). These features were consequently utilized to construct the significant statistical models to rapid and effectively distinguish lignin-utilizing strains, with the accuracy of positive growth of up to 97.3% (Table 1). The accuracy of positive growth reached 100%, when the model was applied to 27 marine bacterial strains isolated in our lab, validating the model's effectiveness (Table 1). In addition, the relatively low accuracy of non-growth

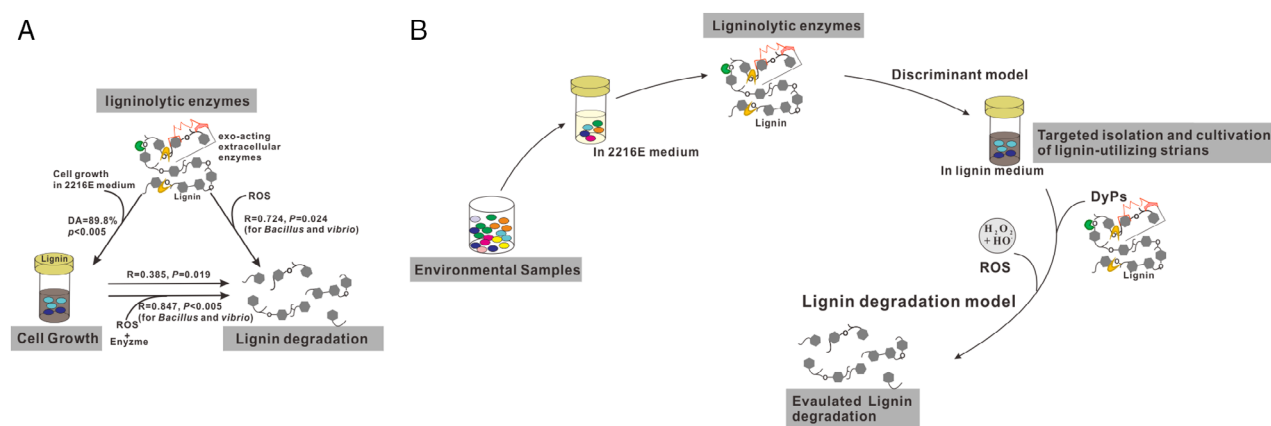


Fig. 5. The relationship of ligninolytic enzymes, ROS, cell growth and lignin degradation in bacterial lignin degradation. A. The links between ligninolytic enzymes, cell growth and lignin degradation in bacterial lignin degradation. DA: The accuracy of discriminant function analysis. B. The strategy for isolation of lignin-utilizing bacteria via the links. Diagram showing the steps in this strategy. Strains from marine environments are cultured in 2216E medium at 30°C to measure their OD600 values and DyP activities. The discriminant model is applied to distinguish lignin-utilizing strains. For *Bacillus* and *Vibrio* lignin-utilizing strains, the linear regression model is applied to rapidly evaluate their capacity of lignin consumption when they are cultured in soluble lignin medium. [Color figure can be viewed at wileyonlinelibrary.com]

(57.1%) should be the result of limited number of non-growth strains in the test set (seven out of 27 strains). As higher accuracy (75%) of non-growth was observed for the 12 strains out of the 49 strains, the accuracy of non-growth would be enhanced with the increment of non-lignin-utilizing marine bacterial strains in the collected samples. Together, this model is suitable to preliminarily screen lignin-utilizing marine bacteria in a high-throughput manner, without requirement of laborious procedures to culture bacteria in lignin mineral medium with longer growth periods, monitor cell growth (as measured by CFUs/ml) and quantify consumed lignin.

Impact on extracellular ligninolytic enzymes for bacterial lignin degradation

To complete global carbon cycling, microorganisms have developed many enzymatic strategies to decompose lignin. It is well-known that white-rot fungi have a rich suite of extracellular oxidative enzymes to degrade lignin, including different types of heme-containing peroxidases [e.g., LiP, MnP, DyP and versatile peroxidases (VP)] and copper-containing oxidative laccases (Floudas *et al.*, 2012). In contrast, bacterial ligninolytic enzymes, especially those of aquatic organisms, have been less well studied (de Gonzalo *et al.*, 2016). This study reveals several novel clues for marine bacterial ligninolytic enzymes. First, ABTS is a more sensitive and specific catalytic substrate to detect the peroxidase activity of DyP, whereas 2, 6-DMP is appropriate to indicate the ligninolytic activity of DyP. ABTS and 2, 6-DMP are commonly utilized substrates to detect DyP activity. However, their differences in indication of enzyme activity are not

yet mentioned. Our study suggested that DyP activity measured by 2, 6-DMP was significantly related to lignin degradation, although the activity measured by ABTS was higher than that measured by 2, 6-DMP (Fig. S6A and B). The ambivalent enzyme activity with different catalytic substrates is possibly the result of variance in catalytic mechanisms. 2, 6-DMP is a monophenolic lignin model, while ABTS is an azo dye (Fig. 4D). Considering that bacterial DyP is generally active on phenolic lignin models (Brown *et al.*, 2012), DyP activity, measured by 2, 6-DMP, should reflect its ligninolytic activity. In addition, in contrast to the phenolic substrate forming quinines and dimmers with C-O and C-C coupling, the oxidation of ABTS proceeds in one step resulting in a single product, the green radical cation ABTS⁺ (Johannes and Majcherczyk, 2000; Adalokun *et al.*, 2012). Thus, calculated enzyme activity, measured by ABTS, was higher than that of 2, 6-DMP. Second, DyP-type peroxidases are the major oxidative enzymes in the degradation of soluble and insoluble lignin, while laccases appear to assist in soluble lignin degradation. Our study suggested that 83.8–100% of strains exhibited DyP activity in soluble and insoluble lignin mineral medium respectively. In contrast, only seven strains (18.9%) with laccase activity in soluble lignin mineral medium and one strain (4%) with laccase activity in insoluble lignin mineral medium were observed. Therefore, the isolated marine bacteria possibly employ DyPs as the primary enzyme for soluble and insoluble lignin degradation, whereas laccases should assist with soluble lignin modification, but are not necessary. Third, ROS is another key factor in a DyP-based enzymatic system, which contributes to bacterial lignin degradation (Fig. 4B). Thus, cell growth,

ROS and DyP enabled us to construct a model to rapidly evaluate the lignin consumption of marine *Bacillus* and *Vibrio* strains, with a 0.85 correlation coefficient. ROS are generated by a variety of ligninolytic accessory enzymes, e.g., H₂O₂-generating oxidases, alcohol oxidases, glucose dehydrogenases and FAD-dependent oxidases (Bissaro *et al.*, 2018), but it is not yet well established which of these are components of the accessory enzymes. Therefore, exploration of these ROS associated enzymes is required to further design a rational strategy for isolation of ligninolytic bacteria as well as understanding the mechanism of bacterial lignin degradation. Finally, the LiPs and MnPs of marine ligninolytic bacteria may not be mainly responsible for lignin degradation. In this study, 67.3% of strains had MnP activity and 57.1% of strains showed LiP activity when these strains were grown in 2216E medium. Unexpectedly, none of the strains showed LiP or MnP activity in the presence of lignin.

Novel marine lignin-utilization bacteria

To date, the marine environment remains relatively unexplored with respect to lignin-degrading bacteria. This study identified several previously unrecognized marine bacterial lignin-degraders of the genera *Yangia*, *Pelagibaca*, *Salipiger*, *Celeribacter* and *Vibrio* (Fig. 1). The former four genera belong to the family *Rhodobacteraceae*, members of which are among the most abundant bacteria in coastal waters and marine sediments (Riedel *et al.*, 2014). Members of *Celeribacter* genera are primarily known for their ability to degrade organic matter. They have mainly been isolated from coastal surface waters and deep-sea sediment and are able to degrade a wide range of polycyclic aromatic hydrocarbons (PAHs) (Cao *et al.*, 2015; Yuan *et al.*, 2015). *Salipiger* species have a versatile carbon source spectrum, including fructose, galactose, maltose, sucrose and glucose (Riedel *et al.*, 2014; Dai *et al.*, 2015). In addition, *Vibrio* species, which are one of dominant microorganisms in the marine environments, are known to utilize a variety of carbon sources, e.g., insoluble chitin, alginate and mannitol (Aunkham *et al.*, 2018; Lim *et al.*, 2019). However, their role in the degradation of terrestrially derived lignin in marine environment had previously been unrecognized. The widely distributed *Rhodobacteraceae* and *Vibrio* strains with lignin-degradation capacity, as revealed by our study, not only improve our understanding of global carbon cycling but also provide new insights for biomass utilization.

In conclusion, this study explores the links between phenotypes of lignin-utilizing bacteria (Fig. 5A). The established discriminant model could rapidly and efficiently distinguish marine lignin-utilizing strains, which

grow in 2216E medium at 30°C (Fig. 5B). Furthermore, we pinpoint lignin utilization is dependent on three important variables, cell growth, ROS and DyP activity (as measured by 2, 6-DMP) and thus proposed a model to evaluate the lignin degradation capacity of *Bacillus* and *Vibrio* strains (Fig. 5B). In the future, the strategy of this application could be expanded to a greater number of lignin-utilizing bacteria over a wider range of niches [e.g., lower (< 10°C) or higher (> 40°C) growth temperature], as well as lignin-degrading bacteria, which can degrade lignin, but are unable utilize it as a carbon source. Our findings are not only valuable in guiding the isolation of lignin-utilizing bacteria, but also offer an example of how to apply physical models to target and culture other bacteria that lack molecular biomarkers or functional gene information, in an effort to fill in the many current gaps in microbial isolation and cultivation.

Experimental procedures

In situ incubation and sample collection

We used three cylindrical polytetrafluoroethylene (PTFE) incubators, each with four chambers (10 cm height and 15 cm in radius) with 1 mm pores. The incubators were filled with *in situ* enrichment medium (10 g agar powder and 5 g phytigel in 1 l artificial seawater) with 3% (wt%) rice straw powder, corn straw powder or wheat straw powder as the sole carbon source respectively. They were deployed in the intertidal zone (122°6'14.05E, 29°56'48.90 N), which is located 50 m from the shoreline of the southern-east of Zhairuoshan Island, Zhejiang Province, China, and fixed to the beach by ropes. After 6 months of incubation (from April 2018 to October 2018), the incubators were recovered. Each 5 g *in situ* enrichment sample was collected, mechanical smashed and resuspended in 45 ml sterilized artificial seawater at 30°C, 200 r.p.m. for 30 min. Subsequently, 5 ml of the mixture was transferred into 100 ml MB medium (0.33 g NaNO₃, 0.88 g NH₄Cl, 0.5 g KCl, 3 g MgCl₂·6H₂O, 0.5 g CaCl₂·2H₂O, 3 g Na₂SO₄, 22 g NaCl, 0.05 g KH₂PO₄, 1 ml trace elements and 1 ml vitamins in 1 l ddH₂O) (Widdel and Bak, 1992) with 3% (wt%) corresponding lignocellulose substrate and incubated at 30°C, 150 r.p.m. for 7 days. Subsequently, 100 µl of culture was collected, appropriately diluted with sterilized artificial seawater, spread onto 2216E agar plates and incubated at 30°C until single colonies were observed.

Strain isolation, identification and cultivation

Two-hundred isolates were picked and underwent several rounds of transfer to fresh 2216E agar plates until pure cultures were obtained. All isolates were cultured in

2216E liquid medium to monitor the growth curve (as measured by OD600) and enzyme activity (laccase, DyP, MnP and LiP) at early-, mid- and late-log phases. Next, each isolate was inoculated in MB medium with 3 g/l of either soluble or insoluble lignin as the sole carbon source. Two types of commercially available lignin were used in this study. According to the suppliers' specifications, the insoluble lignin (catalogue # 370959, Sigma-Aldrich, St Louis, MO, USA) was separated from cellulose (e.g., wood pulp) by hot alkaline (sulfate) method, contained 2% sulfur impurities and had a density of 1.3 g/ml at 25°C (Lin *et al.*, 2019), while the soluble lignin (catalogue # 471003, Sigma-Aldrich, St Louis, MO, USA) was produced by kraft delignification of Norway spruce, contained 4% sulfur impurities and had an average MW of 10 000 Da (Bandounas *et al.*, 2011). The positive-growth isolates in lignin medium were defined as lignin-utilizing strains. The growth curves in lignin medium were monitored by counting CFUs per millilitre on 2216E plates as previously described (Lin *et al.*, 2019). Meanwhile, isolates that showed no growth in lignin medium were defined as non-lignin-utilizing strains and were subsequently cultured in MB medium supplemented with 3 g/l soluble lignin and 1% (w/v) glucose. Their growth curves were also monitored by counting CFUs per millilitre on 2216E agar plates. Strains capable of degrading lignin under these conditions were categorized as lignin-degrading strains. All the growth curves were performed in biological triplicate.

In addition, to test the established physical models, 27 marine bacteria were randomly selected. They were isolated in our lab from a cold spring in South China Sea, the polycyclic aromatic hydrocarbon contaminated coastal area of the East China Sea, and marine sediment from the Pacific Ocean, and cultured in 2216E medium and soluble lignin mineral medium at a speed of 150 rpm, 30 °C respectively. Their growth curves and enzyme activity were monitored as described above. All the growth curves were performed in biological triplicate.

DNA extraction, PCR amplification and phylogenetic analysis of 16S rRNA gene

A single colony from each isolate was transferred to a glass tube with 5 ml 2216E liquid medium and incubated at 30°C for 1–3 days with shaking, 150 r.p.m. The cultured cells were collected to extract genomic DNA as previously described (Lin *et al.*, 2011). The 16S rRNA gene was amplified from genomic DNA of all isolates using a bacterial universal primer set (27F: 5'-AGAGTTTGAT CCTGGCTCAG-3' and 1492R: 5'-TACCTTGTTACGAC TT-3'). The PCR product was purified and Sanger sequenced (Tsinke Bio Company). The obtained DNA

sequences were aligned in GenBank using the BLAST tools to assign taxonomy. After multiple sequence alignment of the sequences by Clustal X and manual correction, a 1400 bp segment was selected to construct a phylogenetic tree via the neighbour-joining method in the MEGA software version 5.0 (Wang *et al.*, 2016).

Extracellular enzyme assays

Enzymatic activity assays were performed at 30°C and monitored by a Synergy 2 microplate reader (BioTek, Vermont, USA). One unit of enzyme activity was defined as the enzyme amount oxidizing 1 µmol substrate per minute. Culture supernatant was collected by centrifuging (13 000 g for 3 min at 4°C) as the crude enzyme. Laccase activity was measured via oxidation of either ABTS (catalogue # A109612, Aladdin, Shanghai, China) or 2, 6-DMP (catalogue # D128348, Aladdin, Shanghai, China) (Johannes and Majcherzyk, 2000). For ABTS, the catalytic reaction was performed in 50 mM acetate buffer (pH 4.5) with 4 mM ABTS and monitored at 420 nm ($\epsilon_{420} = 36\,000\text{ M}^{-1}\text{ cm}^{-1}$) (Nakagawa *et al.*, 2010). For 2, 6-DMP, the catalytic reaction was performed in 50 mM acetate buffer (pH 4.5) with 4 mM 2, 6-DMP and monitored at 469 nm ($\epsilon_{469} = 49\,600\text{ M}^{-1}\text{ cm}^{-1}$). Similarly, DyP-type peroxidase (DyP) activity was detected by the above methods; however, it required 1 mM H₂O₂ to initiate the reaction (Brissos *et al.*, 2017; Lin *et al.*, 2019). Manganese peroxidase (MnP) activity was measured via oxidation of 0.5 mM 2, 6-DMP in 50 mM sodium tartrate buffer (pH 5.0) with 1 mM MnSO₄ and 1 mM H₂O₂ at 469 nm ($\epsilon_{469} = 49,600\text{ M}^{-1}\text{ cm}^{-1}$) (Shi *et al.*, 2013). The lignin peroxidase (LiP) activity assay was performed in 100 mM sodium tartrate buffer (pH 3.0) with 3 mM veratryl alcohol (VA, catalogue # V162979, Aladdin, Shanghai, China) and 1 mM H₂O₂ at 310 nm ($\epsilon_{310} = 9300\text{ M}^{-1}\text{ cm}^{-1}$) (Xu *et al.*, 2018). All enzymatic assays were performed in biological triplicate and technical duplicate.

Lignin concentration assay

To measure soluble lignin concentration, 200 µl cultivation supernatant was collected and then monitored by absorbance at 280 nm to determine the concentrations of residual soluble lignin in the culture medium (Chai *et al.*, 2014). Measurement of insoluble lignin concentration was performed as previously described using the Prussian blue assay (Lin *et al.*, 2019). All experiments were performed in biological triplicate.

ROS assay

The ROS concentration was measured by the reactive oxygen species assay kit (Mingxiu Bio, Shanghai, China). 800 μ l culture supernatant was collected by centrifuging (3000 g for 10 min at 4 °C), mixed with 1 μ l reagent B dye [6-chloromethyl-2', 7'-dichlorodihydrofluorescein diacetate (CM-H2DCFDA)] and incubated at 37°C for 30 min. The fluorescence signals were monitored by Biotek microplate reader (Synergy H1) every 10 min at an excitation wavelength (Ex) of 490 nm and an emission wavelength (Em) of 530 nm for up to 90 min. The maximum rate (V_{max}) of fluorescence increase of each sample was calculated using the formula $V_{max} = \Delta F/\Delta T$ per minute (Volk *et al.*, 2018). ΔF represents the change of fluorescence intensity and ΔT represents the time interval between the selected ranges. Un-inoculated medium was used as blank control. All experiments were performed in biological triplicate. Differences between groups were evaluated using two-tailed unpaired *t*-tests. Those with *p*-values <0.05 were considered significant.

Statistical analysis

All the statistical analyses were performed by the statistical package for social science software IBM SPSS 25.0 (Chicago, IL, USA). The general descriptive statistics was performed for all measurements to provide mean and standard deviation for all samples respectively. Significance among samples was checked using student's *t*-test.

The different enzyme profiles and growth capacity between the positive-growth strains and no growth strains were assessed by discriminant function analysis (Wen *et al.*, 2014). Two processes were applied: (i) multivariate discriminant function analysis, in which all five independent variables were considered, and (ii) stepwise discriminant function analysis, in which the quantitative variables were selected. Subsequently, the discriminant scores of positive (S_p) and negative (S_n) groups were calculated using the discriminant function $S = C_0 + C_1X_1 + C_2X_2 + \dots + C_nX_n$, (C_0 is constant, C_1-C_n are coefficients and X_1-X_n are variables) (Wen *et al.*, 2014). For an unknown sample, its S_p and S_n were calculated respectively. If S_p was higher than S_n , it was considered positive growth, otherwise, it was considered no growth.

To test the accuracy of each discriminant model, the cross-validation classification in each functional process was performed by the leave-one-out classification method (Balog *et al.*, 2013). Briefly, each sample was treated as a validation set, and classified by discriminant functions created by the training set of all individual except itself. Consequently, the accuracy of cross-validation was obtained followed by the above equation.

To calculate the importance of each independent variable, a standardized canonical discriminant function was given for two processes of discriminant analysis respectively (Rencher, 1992). The obtained absolute value of function coefficients of all parameters represents their contribution to the established discriminant model and was defined as factor importance.

Linear regression analysis was conducted as previously described (Lao *et al.*, 2016) to assess the relationship of cell growth, extracellular enzyme activities and lignin degradation when strains were cultured in lignin medium. Correlation coefficient (*R*) was calculated to evaluate the correlation of each group. $R \leq 0.35$ represents low or weak correlation. $0.36 \leq R \leq 0.67$ indicates moderate correlation, while $0.68 \leq R \leq 1.0$ is generally considered high correlation (Mason *et al.*, 1983). Similar to the discriminant model, the standardized coefficients for each independent variable were displayed in the linear regression analysis. The absolute value of function coefficients, which represents their relative contribution to the established regression model, was defined as factor importance in this study.

Acknowledgements

This work was supported by the National Natural Science Foundation of China (91951116) and National Key Research and Development Project (2019YFA0606704). The funders had no role in the study design, data collection and analysis, decision to publish or preparation of the manuscript.

Author contributions

L.L. conceived and designed the experiments. W.X. performed the experiments. L.L. and W.X. analysed the data. L.L. and Z.J. wrote the paper. All authors read and approved the final manuscript.

References

- Adelakun, O.E., Kudanga, T., Green, I.R., Roes-Hill, M.L., and Burton, S.G. (2012) Enzymatic modification of 2,6-dimethoxyphenol for the synthesis of dimers with high antioxidant capacity. *Process Biochem* **47**: 1926–1932.
- Agrawal, K., and Verma, P. (2019) Laccase: addressing the ambivalence associated with the calculation of enzyme activity. *3 Biotech* **9**: 365.
- Aunkham, A., Zahn, M., Kesireddy, A., Pothula, K.R., Schulte, A., Basle, A., *et al.* (2018) Structural basis for chitin acquisition by marine *Vibrio* species. *Nat Commun* **9**: 017-02523.
- Baker-Austin, C., Oliver, J.D., Alam, M., Ali, A., Waldor, M. K., Qadri, F., and Martinez-Urtaza, J. (2018) *Vibrio* spp. infections. *Nat Rev Dis Primers* **4**: 8.
- Balog, J., Sasi-Szabo, L., Kinross, J., Lewis, M.R., Muirhead, L.J., Veselkov, K., *et al.* (2013) Intraoperative

- tissue identification using rapid evaporative ionization mass spectrometry. *Sci Transl Med* **5**: 3005623.
- Bandounas, L., Wierckx, N.J., de Winde, J.H., and Ruijsenaars, H.J. (2011) Isolation and characterization of novel bacterial strains exhibiting ligninolytic potential. *BMC Biotechnol* **11**: 1472–6750.
- Becker, J., and Wittmann, C. (2019) A field of dreams: lignin valorization into chemicals, materials, fuels, and health-care products. *Biotechnol Adv* **37**: 6.
- Bissaro, B., Varnai, A., Rohr, A.K., and Eijssink, V.G.H. (2018) Oxidoreductases and reactive oxygen species in conversion of lignocellulosic biomass. *Microbiol Mol Biol Rev* **82**: 00029-18.
- Brissos, V., Tavares, D., Sousa, A.C., Robalo, M.P., and Martins, L.O. (2017) Engineering a bacterial DyP-type peroxidase for enhanced oxidation of lignin-related phenolics at alkaline pH. *ACS Catal* **7**: 3454–3465.
- Brown, M.E., Barros, T., and Chang, M.C. (2012) Identification and characterization of a multifunctional dye peroxidase from a lignin-reactive bacterium. *ACS Chem Biol* **7**: 2074–2081.
- Brown, M.E., and Chang, M.C. (2014) Exploring bacterial lignin degradation. *Curr Opin Chem Biol* **19**: 1–7.
- Bugg, T.D., Ahmad, M., Hardiman, E.M., and Rahmanpour, R. (2011) Pathways for degradation of lignin in bacteria and fungi. *Nat Prod Rep* **28**: 1883–1896.
- Cao, J., Lai, Q., Yuan, J., and Shao, Z. (2015) Genomic and metabolic analysis of fluoranthene degradation pathway in *Celeribacter indicus* P73T. *Sci Rep* **5**: 7741.
- Chai, L.Y., Chen, Y.H., Tang, C.J., Yang, Z.H., Zheng, Y., and Shi, Y. (2014) Depolymerization and decolorization of Kraft lignin by bacterium *Comamonas* sp. B-9. *Appl Microbiol Biotechnol* **98**: 1907–1912.
- Chen, Y.H., Chai, L.Y., Zhu, Y.H., Yang, Z.H., Zheng, Y., and Zhang, H. (2012) Biodegradation of Kraft lignin by a bacterial strain *Comamonas* sp. B-9 isolated from eroded bamboo slips. *J Appl Microbiol* **112**: 900–906.
- Cross, K.L., Campbell, J.H., Balachandran, M., Campbell, A. G., Cooper, S.J., Griffen, A., et al. (2019) Targeted isolation and cultivation of uncultivated bacteria by reverse genomics. *Nat Biotechnol* **37**: 1314–1321.
- D'Onofrio, A., Crawford, J.M., Stewart, E.J., Witt, K., Gavriš, E., Epstein, S., et al. (2010) Siderophores from neighboring organisms promote the growth of uncultured bacteria. *Chem Biol* **17**: 254–264.
- Dai, X., Shi, X., Gao, X., Liang, J., and Zhang, X.H. (2015) *Salipiger nanhaiensis* sp. nov., a bacterium isolated from deep sea water. *Int J Syst Evol Microbiol* **65**: 1122–1126.
- de Gonzalo, G., Colpa, D.I., Habib, M.H., and Fraaije, M.W. (2016) Bacterial enzymes involved in lignin degradation. *J Biotechnol* **236**: 110–119.
- Floudas, D., Binder, M., Riley, R., Barry, K., Blanchette, R. A., Henrissat, B., et al. (2012) The paleozoic origin of enzymatic lignin decomposition reconstructed from 31 fungal genomes. *Science* **336**: 1715–1719.
- Johannes, C., and Majcherczyk, A. (2000) Laccase activity tests and laccase inhibitors. *J Biotechnol* **78**: 193–199.
- Kharayat, Y., and Thakur, I.S. (2012) Isolation of bacterial strain from sediment core of pulp and paper mill industries for production and purification of lignin peroxidase (LiP) enzyme. *Bioremediat J* **16**: 125–130.
- Lagier, J.C., Khelaifia, S., Alou, M.T., Ndongo, S., Dione, N., Hugon, P., et al. (2016) Culture of previously uncultured members of the human gut microbiota by culturomics. *Nat Microbiol* **1**: 203.
- Lao, P.J., Betthausen, T.J., Hillmer, A.T., Price, J.C., Klunk, W.E., Mihaila, I., et al. (2016) The effects of normal aging on amyloid-beta deposition in nondemented adults with down syndrome as imaged by carbon 11-labeled Pittsburgh compound B. *Alzheimers Dement* **12**: 380–390.
- Lim, H.G., Kwak, D.H., Park, S., Woo, S., Yang, J.S., Kang, C.W., et al. (2019) *Vibrio* sp. dhg as a platform for the biorefinery of brown macroalgae. *Nat Commun* **10**: 019-10371.
- Lin, L., Cheng, Y., Pu, Y., Sun, S., Li, X., Jin, M., et al. (2016) Systems biology-guided biodesign of consolidated lignin conversion. *Green Chem* **18**: 5536–5547.
- Lin, L., Song, H., Tu, Q., Qin, Y., Zhou, A., Liu, W., et al. (2011) The *Thermoanaerobacter* glyco biome reveals mechanisms of pentose and hexose co-utilization in bacteria. *PLoS Genet* **7**: e1002318.
- Lin, L., Wang, X., Cao, L., and Xu, M. (2019) Lignin catabolic pathways reveal unique characteristics of dye-decolorizing peroxidases in *Pseudomonas putida*. *Environ Microbiol* **21**: 1847–1863.
- Mason, R.O., Lind, D.A., and WG, M. (1983) *Statistics: An Introduction*. New York, NY, USA: Harcourt Brace Jovanovich, Inc.
- Nakagawa, Y., Sakamoto, Y., Kikuchi, S., Sato, T., and Yano, A. (2010) A chimeric laccase with hybrid properties of the parental *Lentinula edodes* laccases. *Microbiol Res* **165**: 392–401.
- Nayfach, S., Shi, Z.J., Seshadri, R., Pollard, K.S., and Kyrpides, N.C. (2019) New insights from uncultivated genomes of the global human gut microbiome. *Nature* **568**: 505–510.
- Rencher, A.C. (1992) Interpretation of canonical discriminant functions, canonical variates, and principal components. *Am Stat* **46**: 217–225.
- Riedel, T., Spring, S., Fiebig, A., Petersen, J., Kyrpides, N. C., Goker, M., and Klenk, H.P. (2014) Genome sequence of the exopolysaccharide-producing *Salipiger mucosus* type strain (DSM 16094(T)), a moderately halophilic member of the *Roseobacter* clade. *Stand Genomic Sci* **9**: 1331–1343.
- Salvachua, D., Karp, E.M., Nimlos, C.T., Vardon, D.R., and Beckham, G.T. (2015) Towards lignin consolidated bioprocessing: simultaneous lignin depolymerization and product generation by bacteria. *Green Chem* **17**: 4951–4967.
- Shi, Y., Chai, L., Tang, C., Yang, Z., Zhang, H., Chen, R., et al. (2013) Characterization and genomic analysis of Kraft lignin biodegradation by the beta-proteobacterium *Cupriavidus basilensis* B-8. *Biotechnol Biofuels* **6**: 1.
- Shobharani, P., Padmaja, R.J., and Halami, P.M. (2015) Diversity in the antibacterial potential of probiotic cultures *Bacillus licheniformis* MCC2514 and *Bacillus licheniformis* MCC2512. *Res Microbiol* **166**: 546–554.
- Strachan, C.R., Singh, R., VanInsberghe, D., levdokymenko, K., Budwill, K., Mohn, W.W., et al. (2014) Metagenomic scaffolds enable combinatorial lignin transformation. *Proc Natl Acad Sci U S A* **111**: 10143–10148.

- Vavourakis, C.D., Andrei, A.S., Mehrshad, M., Ghai, R., Sorokin, D.Y., and Muyzer, G. (2018) A metagenomics roadmap to the uncultured genome diversity in hypersaline soda lake sediments. *Microbiome* **6**: 018-0548.
- Velayutham, K., Madhava, A.K., Pushparaj, M., Thanarasu, A., Devaraj, T., Periyasamy, K., and Subramanian, S. (2018) Biodegradation of remazol brilliant blue R using isolated bacterial culture (*Staphylococcus* sp. K2204). *Environ Technol* **39**: 2900–2907.
- Volk, J., Ziemann, C., Leyhausen, G., and Geurtsen, W. (2018) Genotoxic and mutagenic potential of camphorquinone in L5178/TK(+/-) mouse lymphoma cells. *Dent Mater* **34**: 519–530.
- Wang, L., Nie, Y., Tang, Y.Q., Song, X.M., Cao, K., Sun, L.Z., *et al.* (2016) Diverse bacteria with lignin degrading potentials isolated from two ranks of coal. *Front Microbiol* **7**: 1–14.
- Wen, J., Yang, H., Liu, M.Z., Luo, K.J., Liu, H., Hu, Y., *et al.* (2014) Gene expression analysis of pretreatment biopsies predicts the pathological response of esophageal squamous cell carcinomas to neo-chemoradiotherapy. *Ann Oncol* **25**: 1769–1774.
- Widdel, F., and Bak, F. (1992) Gram-negative mesophilic sulfate-reducing bacteria. In *The Prokaryotes: A Handbook on the Biology of Bacteria: Ecophysiology, Isolation, Identification, Applications*, Balows, A. (ed). New York, NY, USA: Springer, pp. 3352–3378.
- Xu, Z., Qin, L., Cai, M., Hua, W., and Jin, M. (2018) Biodegradation of Kraft lignin by newly isolated *Klebsiella pneumoniae*, *Pseudomonas putida*, and *Ochrobactrum tritici* strains. *Environ Sci Pollut Res Int* **25**: 14171–14181.
- Yang, C.X., Wang, T., Gao, L.N., Yin, H.J., and Lu, X. (2017) Isolation, identification and characterization of lignin-degrading bacteria from Qinling, China. *J Appl Microbiol* **123**: 1447–1460.
- Yuan, J., Lai, Q., Sun, F., Zheng, T., and Shao, Z. (2015) The diversity of PAH-degrading bacteria in a deep-sea water column above the Southwest Indian Ridge. *Front Microbiol* **6**: 853.
- Zhao, C., Xie, S., Pu, Y., Zhang, R., Huang, F., Ragauskas, A.J., and Yuan, J.S. (2016) Synergistic enzymatic and microbial lignin conversion. *Green Chem* **18**: 1306–1312.
- Zhou, H., Guo, W., Xu, B., Teng, Z., Tao, D., Lou, Y., and Gao, Y. (2017) Screening and identification of lignin-degrading bacteria in termite gut and the construction of LiP-expressing recombinant *Lactococcus lactis*. *Microb Pathog* **112**: 63–69.
- C. Image of the intertidal zone (122°6'14.05E, 29°56'48.90 N) on the southern-east of Zhairuoshan Island.
- Fig. S2.** The growth curves and enzyme activities in 2216E medium of seven isolates that belong to the *Vibrio* sp. 45 group. Seven strains, which belong to *Vibrio* sp. 45 group, were cultured in 2216E medium. Cell growth (OD600), laccase, LiP, DyP and MnP were measured in real-time. U/L: the total enzyme activity in 1 l batch culture broth.
- Fig. S3.** The growth curves and enzyme activities in 2216E medium of five isolates that belong to the *Bacillus flexus* 81 group. Five strains, which belong to *Vibrio* sp. 45 group, were cultured in 2216E medium. Cell growth (OD600), laccase, LiP, DyP and MnP were measured in real-time. U/L: the total enzyme activity in 1 l batch culture broth.
- Fig. S4.** Phylogenetic tree and carbon utilization patterns of 27 marine strains. All were cultured in 2216E medium and soluble lignin mineral medium respectively. Phylogenetic trees were constructed by the Neighbour-Joining method using full length sequences of the 16S rRNA gene. The percentage of replicate trees is indicated at the branch nodes.
- Fig. S5.** Correlation between lignin degradation and cell growth for the 37 strains capable of growth on soluble lignin. The strains were cultured in soluble lignin.
- Fig. S6.** The associations of DyP-type peroxidase activities in varied cell culture media and enzyme activity assays.
- A. Correlation between DyP-type peroxidase activities in soluble lignin mineral medium as measured by ABTS and 2, 6-DMP assays.
- B. Correlation between DyP-type peroxidase activities in insoluble lignin mineral medium as measured by ABTS and 2, 6-DMP assays.
- C. Correlation between DyP-type peroxidase activities in soluble lignin mineral medium and insoluble lignin mineral medium.
- Table S1.** The growth and extracellular enzyme activity of the 49 representative strains when cultured in 2216E medium.
- Table S2.** The growth and extracellular enzyme activity of the 37 strains that showed growth in soluble lignin mineral medium.
- Table S3.** The growth and extracellular enzyme activity of the 25 strains that showed growth in insoluble lignin mineral medium.
- Table S4.** The growth and extracellular enzyme activity of the 12 strains, incapable of growth in soluble lignin mineral medium, but capable of growth in mineral medium supplemented with soluble lignin and glucose as the carbon sources.
- Table S5.** Means, standard deviations, and *p*-values of the five parameters for the 49 representative strains.
- Table S6.** The growth and extracellular enzyme activity of the 27 tested marine strains when cultured in 2216E medium.
- Table S7.** The growth and extracellular enzyme activity of the 20 tested marine strains that showed growth in soluble lignin mineral medium.

Supporting Information

Additional Supporting Information may be found in the online version of this article at the publisher's web-site:

Fig. S1. Sampling location in the Zhoushan area.

A. and B. A satellite image obtained using Google Maps showing the location used as the enrichment site in this study.